ICAS Proceedings 1996

20th Congress
of the
International Council of the Aeronautical Sciences

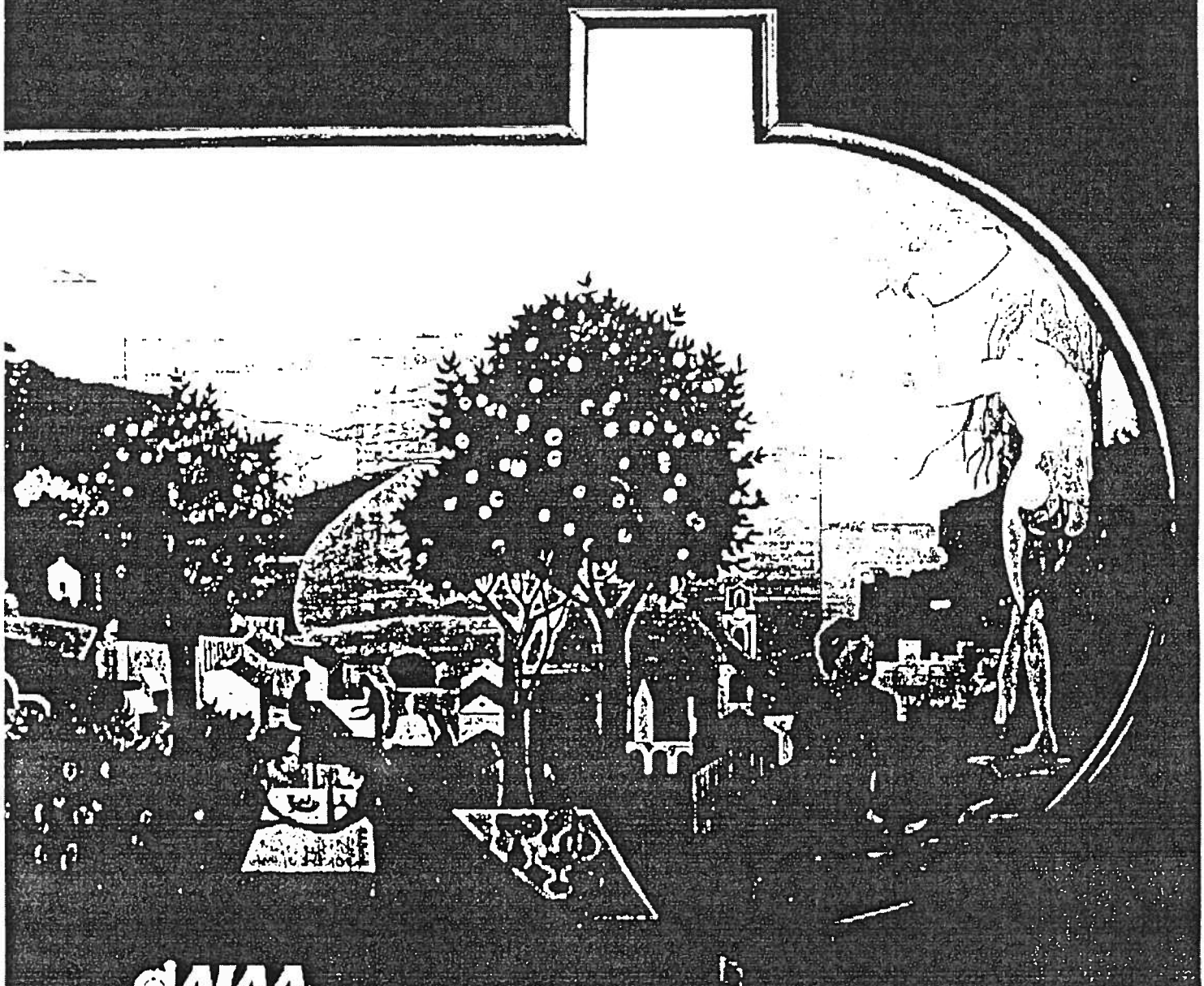

AIAA

Sorrento, Napoli, Italy
8 - 13 September, 1996
Volume 2

DYNAMICS OF ONE-DIMENSIONAL STRUCTURES WITH DESIGNED-IN DISORDER

M. Sayar, M. C. Demirel, and A. R. Atılgan
School of Civil Engineering, Boğaziçi University,
Bebek 80815, Istanbul, Turkey

Abstract

Dynamic characteristics of one-dimensional periodic and nearly periodic structures are investigated. Each substructure has a mass and a grounding stiffness. The connection between substructures are achieved by harmonic and anharmonic nearest neighbor interactions. Harmonic and anharmonic interaction potentials result in linear and nonlinear coupling stiffnesses, respectively, between the substructures. Periodicity is deliberately broken by designing small disorder either in the linear coupling stiffness or in the grounding stiffness. Modal analysis is performed for the linearized behavior of the structure. Principal component analysis is utilized for the nonlinear behavior of the structure which is in thermodynamic equilibrium. It is found that nonlinear interactions delocalize the modes associated with lower frequencies, especially if the disorder is designed in the grounding stiffness.

Introduction

One-dimensional (1D) periodic structures are ubiquitous in the area pertinent to the modeling of engineering structures. A periodic structure contains a modular repeat unit with a mass and a stiffness called grounding stiffness. In 1D periodic structures, repeat units are aligned along a line and connected with springs which may be linear or nonlinear. It was first shown in solid state physics by Anderson[1] that presence of disorder in periodic lattices results in localized eigenstates. Later, Hodges[2] utilized this finding in structural vibrations. The author show that distortion of the strict periodicity of a given continuous structure with a small disorder results in normal mode localization. The reader is referred to the review by Ibrahim[3] for developments within the last decade.

An important consequence of this phenomenon for practical applications would follow if one were to determine under what circumstances disorder has a similar effect to damping in that the propagation of vibrations from the external source is confined. In other words, deliberate utilization of disorder may act as a passive controller.[4] Along the same line of thought, the similarities and differences between disorder and structural damping was explored by Langley[5] by comparing the attenuation factors produced for each case. Statistical investigations were presented by Pierre and his collaborators [6, 7] and references cited therein. Effects of disorder in multispan beams were also undertaken by Pierre[8] and Bendiksen and his collaborators[9] who had also initiated the localization applications in aerospace structures[10] and studied applications on large space structures.[11] Recently, Pierre and his co-worker[12] have taken another path in that they have calculated Lyapunov exponents of the wave transfer matrix of the disordered periodic linear system.

Literature covering studies which are involved in studying effects of nonlinear interactions on the localization is meager. Zaslavsky and his collaborators established an analogy between the disorder in particle chains and dynamical problem of transition to chaos.[13] Vakakis and his co-workers[14] used multiple-scales analysis to show the existence of localized modes due to nonlinearity in the grounding stiffness in a periodic structure with cyclic boundary conditions.

In this study, our main aim is to understand the effect of nonlinearity to the localization behavior observed for the linear 1D periodic structure. Nonlinearity is introduced in the nearest neighbor coupling with the aid of a fourth order interaction potential. The similitude between the modal analysis of the linearized system and the principal component analysis of the nonlinear system[15] is employed. In order to

set the stage for the nonlinear analysis, modal analysis for the linearized system is performed first. A global measure is defined using the linear mode shapes which quantifies the distortion in the eigenvectors (mode shapes) due to disorder in coupling or grounding stiffness. The same form of the measure is preserved for the nonlinear analysis; the linear mode shapes are replaced by the eigenvectors of the covariance matrix. Thus, the effect of nonlinearities are manifested in the comparison of these two measures defined for the linear and for the nonlinear cases. In what follows, first, the model and the methodology employed in this study are clarified. The results obtained from the calculations are then discussed. The main finding is that nonlinearity in the coupling stiffness delocalizes the modes, which are localized due to disorder in the grounding stiffness, associated with the lower frequencies. In addition, nonlinearity in the coupling lessens the amount of distortion which is created by the randomness in the coupling stiffness, again for lower frequencies. Concluding remarks along with the ongoing studies is placed at the end.

Method

In this study, linear and nonlinear dynamics of 1D periodic and nearly periodic structures (Figure 1) are investigated. Nonlinear behavior of the system is achieved by introducing a quartic nearest neighbor interaction potential between the substructures.[16] In the linear coupling case, modal analysis is performed; whereas for the nonlinear coupling analysis, principal component analysis is utilized. First, the linear analysis technique is outlined; after that the methodology followed for the nonlinear analysis is explained.

Linear Coupling of the Substructures

In this case, the system consists of m substructures with equal masses M, and equal grounding stiffnesses k. The interaction between the substructures are accomplished by linear nearest neighbor interactions. Let the coupling stiffness of this interaction be k_c. Both ends of the chain are fixed. Connections of the substructures to the fixed ends are also achieved by the coupling stiffness k_c. In this case, the total energy of the system may be written as

$$E_L = \sum_{i=1}^{m} \frac{1}{2}\frac{p_i^2}{M} + \sum_{i=1}^{m} \frac{1}{2} k q_i^2 + \sum_{i=1}^{m+1} \frac{1}{2} k_c (q_i - q_{i-1})^2 \qquad (1)$$

where $q_0 = q_{m+1} = 0$ due to fixed ends. Here q_i and p_i are the displacement and the momentum of the ith substructure, respectively. In the system, disorder is designed in coupling and in grounding stiffnesses by redistributing these stiffnesses with a uniform random distribution about their mean values which are equal to those of the perfect system. The dynamic characteristics, natural frequencies and the mode shapes, of the perfect and disordered linear system may then be obtained by solving the following eigenvalue problem

$$(-\omega^2 M [I] + [K]) (\Psi) = 0 \qquad (2)$$

where ω is the natural frequency, Ψ is the corresponding mode shape, [I] is the identity matrix and [K] is the stiffness matrix of the whole structure. The stiffness matrix is tridiagonal whose (i-1, i), (i, i), and (i, i+1)th elements are $(-k_{c\,i})$, $(k_{ci} + k_{c\,i+1} + k_i)$, and $(-k_{c\,i+1})$, respectively. For the perfectly periodic system $k_{ci} = k_{c\,i+1}$.

Nonlinear Coupling of the Substructures

In addition to the harmonic, *i.e.*, second order, nearest neighbor interaction in the potential, an anharmonic, fourth order nearest neighbor interaction between the substructures is considered. The total energy of the system can then be written as

$$E_{NL} = E_L + \sum_{i=1}^{m+1} \frac{1}{4} \alpha (q_i - q_{i-1})^4 \qquad (3)$$

where $q_0 = q_{m+1} = 0$ and α is the coefficient related to the nonlinearity. The equations of the motion may be obtained via Hamilton equations, *viz.*,

$$\dot{q}_i = \frac{\partial E_{NL}}{\partial p_i}$$
$$\dot{p}_i = -\frac{\partial E_{NL}}{\partial q_i} \qquad (4)$$

where overdot denotes differentiation with respect to time. The time evolution of each substructure of the system can be obtained by

solving eq 4. Time series obtained for displacements or momenta may be expressed in a matrix of the form[17]

$$A = [a_1\, a_2\, \ldots\, a_n] \qquad (5)$$

Here a_i is the column vector characterizing the instantaneous position or momentum of the structure; it consists of m coordinates of each substructure recorded at time t_i, $1 \le i \le n$. This so-called *trajectory matrix* A is decomposed into the product of three matrices by the *singular value decomposition* technique[18]

$$A_{mxn} = U_{mxm}\, \Sigma_{mxm}\, V^T_{mxn} \qquad (6)$$

Here the subscripts denote the sizes of the matrices, Σ is a diagonal matrix, the elements σ_i of which are called the singular values of A, $1 \le i \le m$.
Using eq 5, one can also obtain the *covariance matrix*[17, 19]

$$C_{mxm} = (1/n)\, A_{mxn}\, A^T_{nxm} = (1/n)\, U_{mxm}\, \Sigma^2\, U^T_{mxm} \qquad (7)$$

where (1/n) is a normalization constant. This representation may be called the spectral decomposition of matrix C. The analysis associated with the spectral decomposition of the covariance matrix is usually called *principal component analysis*. In eqs 6 and 7, U is an orthonormal matrix; it may be called the left singular matrix of the trajectory matrix A or the eigenvector matrix of the covariance matrix C. The columns of which are the left singular vectors of A or, equivalently, the eigenvectors of C. Each left singular vector, or eigenvector, represents a new base vector spanning a *singular direction* of the lower dimensional subspace relevant to the intrinsic dynamics of motion.[17,19-22] The columns of V are the corresponding right singular vectors of A. V is normalized, *i.e.*, $V^TV = I$, where I is the identity matrix. U^TA gives the projections of the instantaneous positions a_i along the new base vectors. The elements of Σ are presented in descending order along the diagonal, as $\sigma_1 \ge \sigma_2 \ge \ldots \ge \sigma_m$. The ith element σ_i represents the amplitude of motion along the ith singular direction.

Using instantaneous momentum, p_i, for each substructure and constructing the covariance matrix with momenta, one can derive the entries of the covariance matrix as

$$C_{ij} = \left\langle p_i \frac{\partial E_{NL}}{\partial p_j} \right\rangle = T\delta_{ij} \qquad (8)$$

where equality takes place if the system reaches equipartition. Here T denotes the absolute temperature in the equilibrium.[23-25] In this case, eigenvalues of the covariance matrix are equal to each other, and they are equal to T. The left singular matrix of A becomes the identity matrix. Therefore, we first employ the instantaneous momentum of the structure and show that the system has reached equipartition. After that, we take the instantaneous position of the structure and perform the decomposition once more with position coordinates so as to identify how the effects of disorder are changed when the nonlinear system is ergodic.

Calculations and Results

A 1D chain consisting of 16 substructures is considered. Both ends of the chain are fixed. Susceptibility of the structure to localization depends on the degree of coupling between the substructures. Weak coupling (low k_c) results in strong localization manifested in the rearrangement of the displacements for each substructure as it may be observed from the eigenvectors of the system. In order to create strong localization, the grounding stiffness, k, and the mass, M, are set to unity, while the coupling stiffness, $k_c = 0.01$.

Three different disordered configurations are designed by uniform random distribution of the grounding or coupling stiffnesses about their mean which are the same as the perfect case. In the first two configurations, the randomness is given to the coupling stiffness, k_c. The last configuration contains the random distribution for the grounding stiffness k. The following ratio is defined so as to measure the degree of randomness: $\mu_{k_c}/m_e(k_c)$. Here μ is the standard deviation with subscripts designating the variable to which randomness is built in, and $m_e(k_c)$ stands for the mean of a variable that is between the parenthesis followed m_e. For the first configuration, which is hereafter

called case (a), this ratio is equal to 0.213, while for the second case, which is hereafter called case (b), the ratio is one half of the first. In the third case, which is hereafter called case (c), on the other hand, the numerical value of the ratio for the first case is preserved satisfying $\mu_{kc}/m_e(k_c) = \mu_k/m_e(k_c)$. The reason for observing this equality is the following: the results indicated that the dynamic characteristics found are insensitive to changes that may be made in the mass of the substructure and they are almost (excluding the differences with three orders of magnitude) insensitive to the value of the grounding stiffness.

The dynamic characteristics, natural frequencies and the associated mode shapes, both of the perfect and of the disordered chains are obtained. Two measures are defined to distinguish the differences between the perfect and disordered configurations, (a), (b), and (c). The first is defined to measure the contribution of each natural frequency to the whole frequency spectrum

$$\kappa_i = \omega_i^2/\mathrm{tr}(\lambda^2) \qquad (9)$$

where ω_i is the natural frequency of the ith mode, λ is the eigenvalue matrix, and tr(.) denotes the trace operation. The second measure calculates the difference created in the eigenvectors (mode shapes) due to disorder

$$e_i = \overline{(\Delta\psi_i^2)}^{1/2}/2\overline{(\psi_i^2)}^{1/2} \qquad (10)$$

where $\Delta\psi_i$ is the difference between the perfect and the disordered eigenvectors probed at each substructure for the ith mode; the overbar, $\overline{(.)}$, denotes the averaging over the substructures. Therefore, e_i, is the average difference for the ith mode.

In Figure 2, κ_i, the normalized frequency spectrum is plotted for the four different configurations; perfect, and three disordered configurations, (a), (b), and (c). It may be observed from the figure that the perfect frequency spectrum is not distorted due to randomness in coupling or in grounding stiffnesses. Due to low coupling stiffness, the frequency band of the spectrum is very much narrow in that the highest frequency differs from the lowest one by only five percent. Only observable difference between the perfect and the random case occurs for the case (a) where the randomness is given to the coupling stiffness. The most pronounced difference is at the highest end of the spectrum. Weaker disorder for coupling stiffness and disorder in the grounding stiffness do not produce significant differences from the perfect frequency spectrum.

In Figure 3, e_i, the averaged normalized RMS differences of the eigenvectors for each mode from the perfect case are shown for three disordered configurations, (a), (b), and (c). Despite the insensitivity observed to the disorder in the frequency spectrum, the eigenvector distributions are affected by the randomness in the coupling stiffness, cases (a) and (b), and in the grounding stiffness, case (c). In curve (a), the disorder is in the coupling stiffness with $\mu_{kc}/m_e(k_c) = 0.213$. It may be deduced that the lower modes are not changed as much as the higher modes. Approximately a linear trend of degree of distortion from the lower to the higher modes is observed from the figure. The associated eigenvector distributions for each mode along the substructure confirm this observation. The most localized modes are those associated with the highest end of the frequency spectrum. In curve (b), the randomness is again in the coupling stiffness with one half of the $\mu_{kc}/m_e(k_c)$ ratio used in the curve (a). It is seen that the linearly increasing trend in the deformity of the eigenvector distribution may not be observed any more. The most localized modes are still associated with the highest frequencies, however, the deformity in the eigenvectors associated with the lower frequencies are decreased. In curve (c), the disorder is created in the grounding stiffness, k, with $\mu_{kc}/m_e(k_c) = \mu_k/m_e(k_c)$. In contrast with the first two case, the distortions for the eigenvector distribution take place for the modes related both with the lower end and with the higher end of the frequency spectrum. Symmetry is broken in the curve (c) due to the coupling stiffness. The results displayed in Figure 3 are obtained by averaging over eight different configurations for each curve. Different configurations are created by taking eight different seed numbers while distributing uniform random variables for the stiffnesses in the cases (a), (b), and (c). Note that for each configuration μ/m_e ratio is still constant.

Next, a small nonlinearity with a fourth order potential between the nearest neighbors is added to the energy, which is given by eq 3. The coefficient pertinent to the nonlinearity, α, is selected to be one order of magnitude less than the coupling stiffness k_c so that $\alpha = 0.001$. The nonlinear system with 16 substructures is integrated numerically by the Bulirsch-Stoer method.[26] With this integration scheme, the total energy of the system is preserved up to eight digits during the simulation at each time step. The system is integrated until the equipartition is reached. Thus, the nonlinear analysis is performed on the equilibrated structure.

In Figure 4, in similitude with Figure 2, the normalized spectrum of the eigenvalues of the covariance matrix (or, equivalently, singular values of the trajectory matrix) is displayed. Here, the logarithm of the normalized singular spectrum is plotted so as to display the deviations of the higher singular values from zero. To calculate the numbers in the figure, ω_i is replaced by σ_i, and λ is replaced by Σ in eq 9. The same four configurations as in the linearly coupled substructures is considered. No random distribution is considered for the nonlinearity coefficient. It may be seen from the figure that the normalized spectrum of the singular values are insensitive to the disorder fabricated in the system as in the normalized spectrum of the natural frequencies in the linearly coupled substructures. The contribution of the first, second, and the third singular modes to the whole singular spectrum is 60, 16, and 7 percent, respectively.

In Figure 5, the averaged normalized differences in the left singular vector (or, equivalently, the eigenvector of the covariance matrix) from the perfect case for each mode is shown for three disordered configurations, (a), (b), and (c). To calculate the numbers in the figure, $\Delta\psi_i$'s in eq 10 are now the left singular vectors pertinent to each singular mode. Although the singular spectrum is not affected by the deviations from the perfect structure, the randomness in the coupling stiffness and in the grounding stiffness do affect the singular vector distributions. In parallelism with Figure 3, in curve (a), the disorder is in the coupling stiffness with $\mu_{kc}/m_e(k_c) = 0.213$. It may be inferred that the lower modes are not changed as much as the higher modes like in the linear coupling case. A linear trend of degree of distortion from the lower to the higher modes can be observed until the very end of the modal spectrum. An immediate jump in the distortion takes place at mode number 15. However, the overall degree of distortion is lower than the linear case, which may be found from the scaling of the figure margins.

In Figure 5, the other two cases, too, both qualitatively and quantitatively differ from Figure 3. In curve (b), the randomness is in the coupling stiffness with one half of the $\mu_{kc}/m_e(k_c)$ ratio used in the curve (a). It is seen that the increasing trend in the distortion of the eigenvector distributions from the perfect case is not preserved when the nonlinearity is added. The increase in the distortion is achieved until the mid-spectrum, after that it stays approximately constant. Thus, for lower $\mu_{kc}/m_e(k_c)$ ratio, the number of localized modes broadens along the higher half of the modal spectrum. Another enchanting difference from the linear coupling takes place in the third configuration. In curve (c), the disorder is created in the grounding stiffness, k, with $\mu_k/m_e(k_c) = \mu_{kc}/m_e(k_c)$. It may be recognized that the localized modes obtained at the lower end of the frequency spectrum in the linear coupling case disappear for the nonlinearly coupled substructures. In other words, perfect nonlinear coupling between the substructures delocalizes the modes at the lower end of the spectrum which are created by the random grounding stiffness configuration with linear coupling of substructures. In addition, the most pronounced distortion from the perfect case occurs not at the very end, but some distance to the end of the spectrum. Not shown in this work, the same qualitative picture as in curve (c) of Figure 4 is also obtained when random distribution is considered for the mass of substructures. Note that Figure 5 is not obtained by averaging over different configurations as opposed to Figure 3. However, from preliminary calculations, it is noticed that some smoothing in each curve will take place not invalidating the conclusions drawn here. Not also displayed here, it is also found that longer chains with higher number of substructures behave similarly.

Concluding Remarks

In this study, two different measures are introduced to quantify the differences in dynamic behavior between perfectly periodic and nearly periodic structures in which a small randomness is designed. For linearly coupled substructures, the first measure is related to the contribution of each natural frequency to the whole frequency spectrum. The second measure is associated with the mode shapes. For each mode, it evaluates the RMS distortion of the mode shape of the disordered structure from that of the perfect one. For nonlinearly coupled structures, the same measures may be used with different physical parameters pertinent to the mechanics of the problem. In the nonlinear case, eigenvalue problem of the characteristic matrix is needed to be converted to that of the covariance matrix which consists of the displacements of the structure. Note that the covariance matrix is obtained when the structure reaches equipartition. Thus, for the nonlinear case, natural frequencies are replaced by the eigenvalues of the covariance matrix for the first measure; mode shapes are replaced by the eigenvectors of the covariance matrix for the second measure.

It is found that the first measure, related with the eigenvalues, cannot distinguish the differences between the periodic and disordered structures both in linear and in nonlinear structure. However, the second one, related with the eigenvectors, do reflect the changes made in the structure. The results obtained from the second measure indicated that nonlinear nearest neighbor interactions delocalizes the modes corresponding to lower frequencies. The most pronounced delocalization occurs if the localized modes for the linear structure is obtained by designed-in disorder in the grounding stiffness. In addition, nonlinearity keeps the distortion almost constant at the higher half of the frequency spectrum for weaker randomness given to coupling stiffnesses. As far as ongoing studies are concerned, the equilibrium probability distributions have already been calculated; the entropic differences are now being evaluated. Concurrently, forced response of the linear and nonlinear structures are being studied. In the forced response analysis for structures which are perfectly periodic and with small disorder, the susceptibility in the statistical-mechanical sense is our additional measure to be investigated.

Acknowledgments

Time evolution of the systems that reach equipartition is performed with the aid of the computational facilities (*Silicon Graphics Challenge L* with R4000) of the Polymer Research Center at Boğaziçi University. Stimulating discussions with the members of the Center are gratefully acknowledged. Partial support is provided by the Boğaziçi University Research Funds.

References

[1] P. W. Anderson Reviews of Modern Physics, 50, 191 – 201 (1978).
[2] J. H. Hodges J. Sound Vib., 82, 411-424 (1982).
[3] R. A. Ibrahim Applied Mechanics Reviews, 40, 309 – 328 (1987).
[4] A. H. Nayfeh and M. A. Hawwa AIAA J., 32, 2131-2133 (1994).
[5] R. S. Langley J. Sound Vib., 178, 411-426 (1994).
[6] C. Pierre J. Sound Vib., 139, 111-132 (1990).
[7] P. D. Cha and C. R. Morganti AIAA Journal, 32, 2269 – 2275 (1994).
[8] C. Pierre, D.-M. Tang, and E. H. Dowell AIAA Journal, 25, 1249 – 1257 (1987).
[9] S. D. Lust, P. P. Friedmann, and O. O. Bendiksen AIAA Journal, 31, 348 – 355 (1993).
[10] O. O. Bendiksen, "Aeroelastic Stabilization by Disorder and Imperfections," presented at 16th IUTAM Congress of Theoretical and Applied Mechanics, Lyngby, Denmark, 1984.
[11] O. O. Bendiksen AIAA Journal, 25, 1241 – 1248 (1987).
[12] M. P. Castanier and C. Pierre Journal of Sound and Vibration, 183, 493 – 515 (1995).
[13] V. V. Beloshapkin, A. G. Tretyakov, and G. M. Zaslavsky Communications on Pure and Applied Mathematics, 47, 39 – 46 (1994).
[14] A. Vakakis, T. Nayfeh, and M. King Journal of Applied Mechanics, 60, 388 – 397 (1993).
[15] H. Tong Physica D, 58, 299 - 303 (1992).
[16] G. Benettin, "Ordered and Chaotic Motions in Dynamical Systems with Many Degreesof Freedom," presented at Molecular-Dynamics Simulation of Statistical-Mechanical Systems, Varenna, Italy, 1985.
[17] T. D. Romo, J. B. Clarage, D. C. Sorensen, and G. N. Phillips Proteins: Structure, Functions, and Genetics, 22, 311 (1995).

[18] G. H. Golub and C. F. Van Loan, *Matrix Computations*: Johns Hopkins University Press, 1989.
[19] A. Amadei, A. B. M. Linssen, and H. J. C. Berendsen Proteins: Structure, Function, and Genetics, 17, 412 - 425 (1993).
[20] D. Oh and Y. Park Mech. Syst. Signal Process., 8, 63 - 79 (1994).
[21] M. A. Ozbek, S. Y. Liu, J. T. Gordon, D. S. Newman, and A. R. Atilgan, "Chaotic Vibration in Aircraft Braking Systems," presented at Design Engineering Technical Conferences, 15th Biennial Conference on Mechanical Vibration and Noise, Boston, MA, 1995.
[22] G. Rowlands and J. C. Sprott Physica D, 58, 251 - 259 (1992).
[23] V. L. Berdichevsky, E. Mueller, M. A. Ozbek, and I. Shecktman, "Statistical Properties of Nonlinear Vibrations of Elastic Beams," presented at Fifth Conference on Nonlinear Vibrations, Stability and Dynamics of Structures, VPI, Blacksburg, VA, 1994.
[24] V. L. Berdichevsky, M. A. Ozbek, and W. W. Kim Journal of Applied Mechanics, 61, 670-675 (1994).
[25] V. L. Berdichevsky, W. W. Kim, and M. A. Ozbek Journal of Sound and Vibration, 179, 151-164 (1995).
[26] W. H. Press, S. A. Teukolsky, W. T. Vetterling, and B. P. Flannery, *Numerical Recipes*, Second Edition ed: Cambridge University Press, 1992.

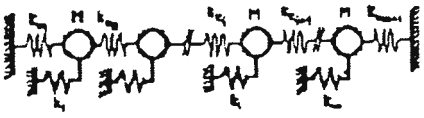

Figure 1. One-dimensional nearly periodic structure with m substructures. Each substructure has a mass M and grounding stiffness k_i. Substructures are connected with linear or nonlinear coupling stiffness, k_{ci}.

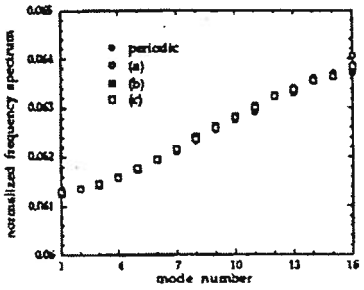

Figure 2. Normalized natural frequency spectrum for perfect and disordered structures calculated by eq 9. Please see the text for definitions of the disordered configurations (a)-(c).

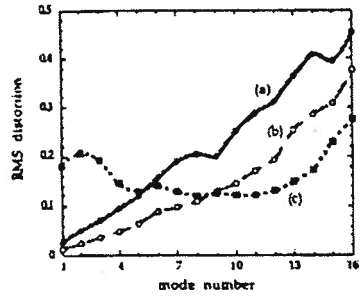

Figure 3. RMS deviations of the eigenvectors from the perfect case calculated using eq 10 for each mode. Curves (a), (b) and (c) represent three disordered configurations.

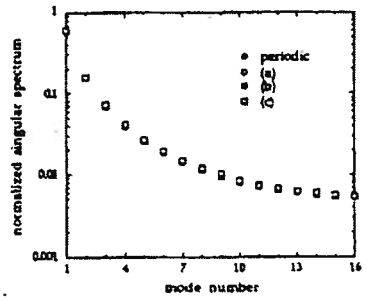

Figure 4. Normalized singular value spectrum for perfect and disordered structures calculated by eq 9 for three disordered configurations (a)-(c).

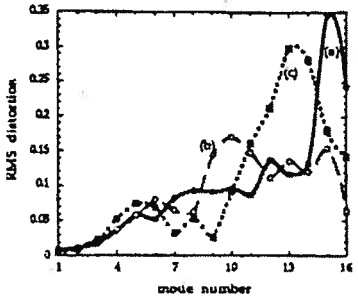

Figure 5. RMS deviations of the eigenvectors of the covariance matrix from the perfect case calculated using eq 10 for each mode. Curves (a), (b) and (c) represent three disordered configurations.